Molecular Cell
Article

Cell Press

Mst1 Promotes Cardiac Myocyte Apoptosis through Phosphorylation and Inhibition of Bcl-xL

Dominic P. Del Re,[1] Takahisa Matsuda,[1] Peiyong Zhai,[1] Yasuhiro Maejima,[1] Mohit Raja Jain,[2] Tong Liu,[2] Hong Li,[2] Chiao-Po Hsu,[3] and Junichi Sadoshima[1,*]

[1]Department of Cell Biology and Molecular Medicine, Cardiovascular Research Institute, Rutgers New Jersey Medical School, Newark, NJ 07103, USA
[2]Center for Advanced Proteomics Research, Rutgers New Jersey Medical School, Newark, NJ 07103, USA
[3]Division of Cardiovascular Surgery, Department of Surgery, Taipei Veterans General Hospital, National Yang-Ming University School of Medicine, Taipei, Taiwan, Republic of China
*Correspondence: sadoshju@njms.rutgers.edu
http://dx.doi.org/10.1016/j.molcel.2014.04.007

SUMMARY

The Hippo pathway, evolutionarily conserved from flies to mammals, promotes cell death and inhibits cell proliferation to regulate organ size. The core component of this cascade, Mst1 in mammalian cells, is sufficient to promote apoptosis. However, the mechanisms underlying both its activation and its ability to elicit cell death remain largely undefined. We here identify a signaling cassette in cardiac myocytes consisting of K-Ras, the scaffold RASSF1A, and Mst1 that is localized to mitochondria and promotes Mst1 activation in response to oxidative stress. Activated Mst1 phosphorylates Bcl-xL at Ser14, which resides in the BH4 domain, thereby antagonizing Bcl-xL-Bax binding. This, in turn, causes activation of Bax and subsequent mitochondria-mediated apoptotic death. Our findings demonstrate mitochondrial localization of Hippo signaling and identify Bcl-xL as a target that is directly modified to promote apoptosis.

INTRODUCTION

Regulation of organ size is of fundamental importance in multicellular organisms. The identification and subsequent elucidation of the Hippo signaling pathway has established this mechanism as a potent negative regulator of organ size and tumorigenesis (Pan, 2010). Hippo mediates these effects through the inhibition of cell growth and proliferation and the induction of apoptosis (Zhao et al., 2011). Indeed, the core mammalian component of this cascade, Mst1, is known to promote apoptosis (Graves et al., 1998), yet the underlying mechanism remains elusive. Furthermore, how and where Mst1 is engaged and activated is still largely unknown.

The *Ras association domain family* (RASSF) polypeptides have been linked to the Hippo signaling pathway and interact with activated Ras GTPases (Avruch et al., 2009; Del Re et al., 2010). Ras proteins are molecular switches that transduce signals to regulate diverse responses including growth, prolifera-

tion, and cell survival (Karnoub and Weinberg, 2008). Their activation status is dependent upon GTP/GDP binding, and downstream signaling is initiated through association with effector proteins. The prototypical isoforms H-Ras and K-Ras4b (hereafter referred to as K-Ras) are ubiquitously expressed; however, differences in subcellular localization and downstream signaling have been demonstrated (Hancock, 2003). Furthermore, *Hras*-null mice are healthy and viable (Esteban et al., 2001), whereas homozygous *Kras* deletion is embryonic lethal (Johnson et al., 1997), indicating nonredundancy between the two. Importantly, the ability of each isoform to engage the Hippo pathway is not known.

Bcl-2 family proteins regulate apoptosis through protein-protein interactions. Upon activation, the executioners Bax and Bak target the mitochondria outer membrane and elicit its permeabilization, thereby releasing apoptogenic factors into the cytosol (Gavathiotis et al., 2010). Bax and Bak are antagonized by the prosurvival family members (e.g., Bcl-2 and Bcl-xL) and activated either directly or indirectly by the BH3-only members (Bad, Bim, and Bid among others) (Chipuk et al., 2010). Several hypotheses have been proposed to explain how, where, and when Bcl-2 family proteins interact to modulate apoptosis, yet the precise mechanism remains controversial (Moldoveanu et al., 2014). Furthermore, crosstalk between Hippo signaling and Bcl-2 family proteins has not been explored.

RESULTS

Ras Activation by Oxidative Stress

Our previous work demonstrated that Hippo signaling is stress-activated in the heart and promotes apoptosis in cardiac myocytes making it a suitable and relevant system to study this pathway (Odashima et al., 2007; Yamamoto et al., 2003). To examine whether H- and K-Ras regulate Mst1, we first precipitated GTP-Ras from hearts subjected to sham operation or ischemia and reperfusion (I/R) and probed with isoform-specific antibodies. We observed a clear increase in GTP-K-Ras, and to a lesser extent GTP-H-Ras, as well as activation of AKT and ERK1/2 following I/R (Figures 1A and 1B). Time course experiments demonstrated rapid activation of K-Ras within 5 min of reperfusion, while H-Ras activation occurred more slowly (Figures S1A and S1B available online). Ras proteins can be oxidized, thereby
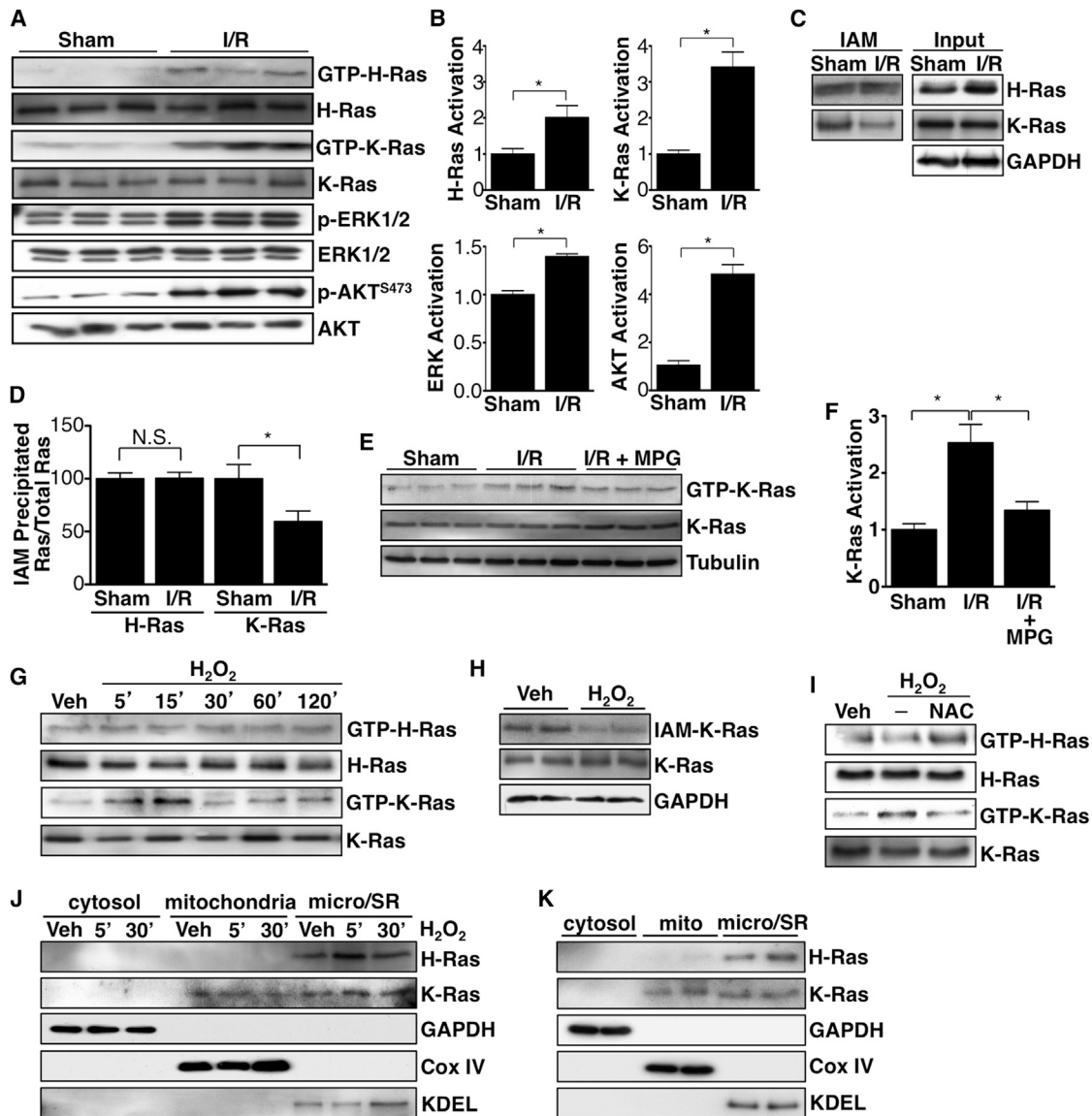
Figure 1. Ras Isoform Activation by Oxidative Stress

(A) Representative immunoblot showing GTP-loaded H- and K-Ras isoforms and phosphorylation of AKT and ERK1/2 from WT mouse heart extracts. Mice were subjected to sham or I/R (30′/60′).

(B) Quantitation of Ras activation and AKT and ERK1/2 phosphorylation immunoblot results; n = 4 for each group. *p < 0.05.

(C) Representative immunoblot demonstrating decreased biotinylated iodoacetamide (IAM) labeling of K-Ras in the mouse heart following I/R.

(D) Quantitation of IAM pulldown experiments; n = 4 for each group. *p < 0.05. N.S., not significant.

(E) Representative immunoblot showing I/R-induced K-Ras activation in the absence and presence of N-2-mercaptopropionyl glycine (MPG). MPG (100 mg/kg) was injected intraperitoneally 24 hr and 1 hr prior to occlusion. Mice were subjected to sham or I/R (30′/60′) and GTP-loaded K-Ras was examined by RBD pulldown.

(F) Quantitation of K-Ras activation results; n = 3 for each group. *p < 0.05. Data are represented as mean ±SEM.

(G) Time course of H- and K-Ras activation in cultured neonatal cardiac myocytes in response to H_2O_2 (100 μM) treatment.

(H) Representative immunoblot demonstrating decreased biotinylated iodoacetamide (IAM) labeling of K-Ras in cardiac myocytes following H_2O_2 (100 μM) treatment (30 min).

(I) The effect of NAC pretreatment (30 min, 5 mM) on Ras isoform activation by H_2O_2 (100 μM; 15 min) in cardiac myocytes.

(J) Representative immunoblot demonstrating subcellular localization of H- and K-Ras in cardiac myocytes.

(K) Localization of endogenous H- and K-Ras in mouse ventricular extracts. GAPDH, Cox IV, and KDEL served as markers of cytosol-, mitochondria-, and microsome/SR-enriched fractions, respectively. See also Figure S1.

promoting their activation (Lander et al., 1995). Because reperfusion following ischemia increases reactive oxygen species (Simpson and Lucchesi, 1987), we hypothesized that myocardial Ras proteins may be oxidized during I/R. We incubated heart extracts from sham- and I/R-operated wild-type (WT) mice with biotinylated iodoacetamide (IAM), which reacts with reduced/free thiols, and precipitated labeled proteins with streptavidin agarose. Probing for K-Ras revealed a significant decrease, indicating cysteine oxidation following I/R, while no significant difference in H-Ras labeling was observed (Figures 1C, 1D, and S1C). Furthermore, treatment of mice with the antioxidant N-2-mercaptopropionyl glycine (MPG) prior to I/R was sufficient to significantly inhibit K-Ras activation (Figures 1E and 1F). These data indicate that K-Ras is oxidized and activated by I/R in the heart.

To determine the cell-autonomous nature of Ras activation, we employed a neonatal rat cardiac myocyte culture. Cardiac myocytes were treated with H_2O_2, and a time course of Ras activation revealed a striking difference between isoforms in response to oxidative stress. The level of GTP-H-Ras did not increase after acute H_2O_2 treatment (5–120 min), whereas K-Ras activation was significantly increased (maximal at 15 min) (Figure 1G). Moreover, K-Ras IAM labeling was decreased by H_2O_2, and pretreatment with the antioxidant N-acetyl cysteine (NAC) attenuated H_2O_2-induced activation of K-Ras, suggesting its activation in cardiac myocytes is dependent upon oxidation (Figures 1H and 1I). Interestingly, treatment with the hypertrophic peptide angiotensin II (Ang II) caused H-Ras, but not K-Ras, activation, suggesting different mechanisms of action between oxidative stress and agonist stimulation (Figure S1D).

H- and K-Ras isoforms are highly conserved but contain C-terminal hypervariable domains leading to different posttranslational modifications that influence subcellular localization (Karnoub and Weinberg, 2008). We hypothesized that subcellular localization may be responsible for the differences observed in activation following oxidative stress. We generated cytosol-, mitochondria-, and microsome/sarcoplasmic reticulum (SR)-enriched fractions from cardiac myocytes. We found predominant localization of H-Ras in the microsome/SR-enriched fraction, whereas K-Ras was detected in both the microsome/SR- and mitochondria-enriched fractions under basal and oxidative stress conditions (Figure 1J). K-Ras in mitochondria-enriched fractions was confirmed in vivo using mouse heart tissue (Figure 1K). On the other hand, we did not detect K-Ras in mitochondria-enriched fractions of HEK293, COS-7, or C2C12 cell lines (Figures S2A, S2B, and S2D), suggesting that H- and K-Ras have distinct subcellular locations in cardiac myocytes.

K-Ras Engages RASSF1A and Activates Mst1

To examine downstream signaling elicited by Ras isoforms, we expressed activated myc-tagged H- and K-Ras12V in cardiac myocytes. H-Ras expression caused increased AKT and ERK1/2 phosphorylation but did not activate the proapoptotic kinase Mst1 (Figures 2A and 2B). Conversely, K-Ras induced AKT and ERK1/2 activation less robustly than H-Ras but elicited clear activation of Mst1 and coimmunoprecipitated with Mst1 in cardiac myocytes (Figures 2A–2C). No difference in signaling between H- and K-Ras was observed in HEK293 or C2C12 cells (Figures S2C and S2E). Although Mst1 is the core component of

the Hippo cascade, no effect on the downstream targets Lats2 or Yap was observed in response to K-Ras (Figure S2F). To further examine this divergence in signaling, cardiac myocytes expressing either isoform were subjected to immunoprecipitation and subsequently probed for the Ras effectors p110α (Rodriguez-Viciana et al., 1994), Raf-1 (Moodie et al., 1993; Vojtek et al., 1993; Warne et al., 1993; Zhang et al., 1993), and RASSF1A (Vos et al., 2000). While active H-Ras was found to associate with p110α and Raf-1, no interaction was observed between H-Ras and RASSF1A (Figure 2D). Interestingly, we saw a clear association between active K-Ras and RASSF1A, but we did not detect p110α or Raf-1 in K-Ras-precipitated samples (Figure 2D). We recently demonstrated that RASSF1A is a regulator of Mst1 activation in the heart (Del Re et al., 2010) and therefore sought to determine whether RASSF1A is involved in K-Ras-induced Mst1 activation. Knockdown of endogenous RASSF1A impaired the ability of K-Ras to promote Mst1 activation, indicating RASSF1A involvement (Figure 2E). We also subjected mice to sham or I/R, precipitated endogenous H- or K-Ras from heart extracts, and then probed for RASSF1A and Mst1. We did not observe an association between RASSF1A or Mst1 and H-Ras in either sham or stressed hearts. However, RASSF1A and Mst1 were detected in samples immunoprecipitated for K-Ras and increased association was observed following I/R (Figure 2F). These findings demonstrate an isoform-specific interaction between endogenous K-Ras, RASSF1A, and Mst1 and indicate an increased association in response to oxidative stress.

Due to the known protective roles of AKT and ERK1/2 in the heart (Lips et al., 2004), we reasoned that H-Ras serves a prosurvival function in cardiac myocytes. We found that active H-Ras significantly protected cardiac myocytes from H_2O_2-induced apoptosis compared to LacZ control. This response was sensitive to the PI3K inhibitor LY294002 or the MEK1 inhibitor PD098059, implicating AKT and MEK1-ERK1/2 involvement (Figure 2G). Strikingly, we observed that active K-Ras expression alone was sufficient to induce apoptosis of cardiac myocytes. This response was significantly attenuated by concomitant knockdown of endogenous RASSF1A or Mst1 or coexpression of a kinase inactive (K59R) Mst1 mutant (Dn-Mst1) (Figures 2H and S2G). Furthermore, we found that H_2O_2-induced apoptosis was attenuated by K-Ras knockdown, while increased K-Ras expression augmented the H_2O_2 apoptotic effect (Figures S2H and S2I). Taken together, these data demonstrate that H-Ras protects cardiac myocytes through activation of AKT and ERK1/2 while K-Ras induces cell death via Mst1.

RASSF1A Mediates Mitochondrial Translocation of Mst1

Our data suggest that differences in subcellular localization of Ras isoforms may mediate divergent signaling and subsequent cellular outcomes. We next examined subcellular localization of Mst1. At baseline, endogenous Mst1 was predominant in the cytosol-enriched fraction (Figure 3A). H_2O_2 treatment elicited translocation of Mst1 to the mitochondria-enriched fraction. Phosphorylated Mst1 increased after H_2O_2 treatment and was found primarily in mitochondria-enriched fractions (Figures 3A, 3B, and S3A). RASSF1A was detected in mitochondria-enriched fractions (Figure 3A), effectively placing
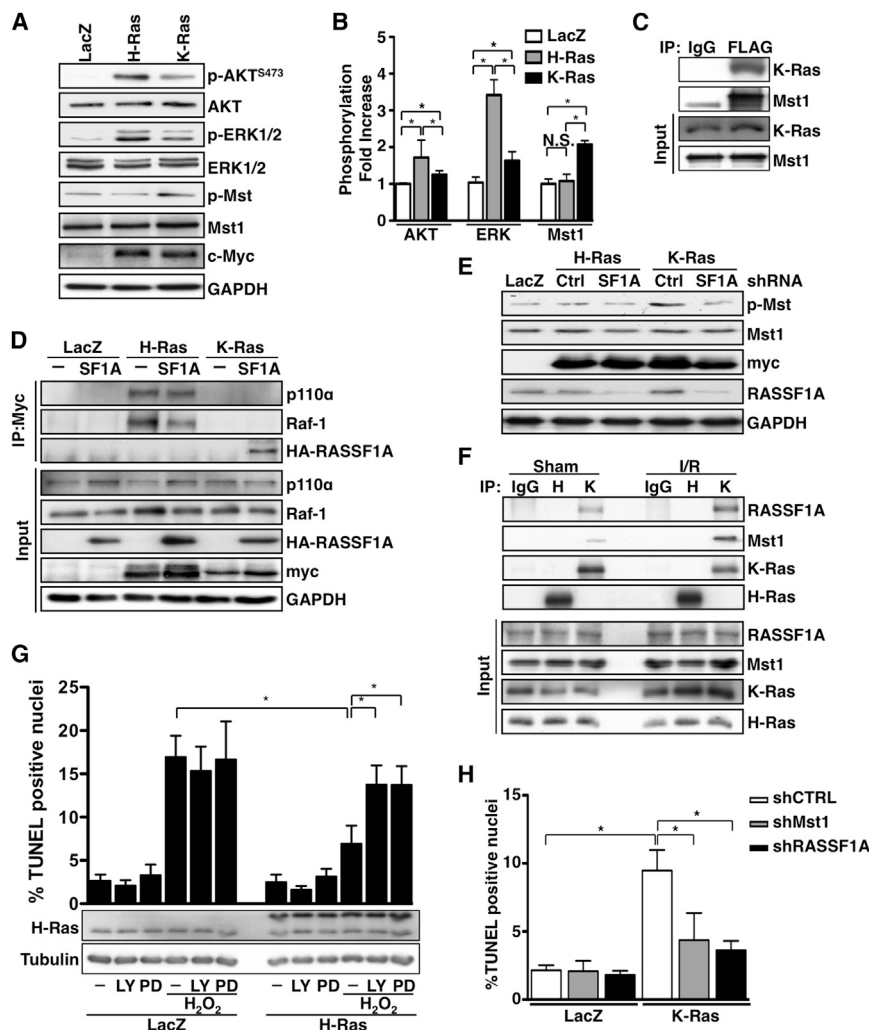
Figure 2. Ras Isoform Signaling

(A) Phosphorylation of AKT, ERK1/2, and Mst1 elicited by H-Ras12V and K-Ras12V adenoviral expression in cardiac myocytes.

(B) Quantitation of immunoblot results. Values are normalized to respective total protein expression; n = 4 for each treatment. *p < 0.05.

(C) Representative immunoblot demonstrating the interaction of endogenous K-Ras with FLAG-Mst1 by coimmunoprecipitation in cardiac myocytes.

(D) Representative immunoblot demonstrating preferential interaction of Ras isoforms with downstream effectors p110α (PI3K), Raf-1, and RASSF1A. Myocytes were infected with LacZ, myc-H-Ras12V, or myc-K-Ras12V in the presence or absence of HA-RASSF1A adenovirus, and immunoprecipitations were performed using anti-c-myc antibody.

(E) Cardiac myocytes were transduced with LacZ, myc-H-Ras12V, or myc-K-Ras12V in combination with scrambled control (Ctrl) or RASSF1A-targeted (SF1A) shRNA adenovirus.

(F) WT mice were subjected to sham or I/R injury (30'/60'), and heart extracts were subjected to immunoprecipitation using H-Ras, K-Ras, or control IgG antibody.

(G) Cardiac myocytes were transduced with LacZ or myc-H-Ras12V adenovirus and treated with vehicle, LY294002 (10 μM), or PD98059 (10 μM) to inhibit PI3K and MEK1, respectively, 30 min prior to addition of H₂O₂ (100 μM). TUNEL was performed 6–8 hr later; n = 3. *p < 0.05.

(H) Cardiac myocytes were transduced with LacZ or myc-K-Ras12V in combination with shCTRL, shMST1, or shRASSF1A adenovirus, and TUNEL was performed 48–72 hr later; n = 3. *p < 0.05. Data are represented as mean ±SEM. See also Figure S2.

K-Ras, RASSF1A, and Mst1 at mitochondria following oxidative stress.

To determine the involvement of RASSF1A in Mst1 translocation, we expressed either WT or a SARAH domain point mutant (L308P) of RASSF1A, which is unable to bind Mst1 (Del Re et al., 2010). We found that endogenous Mst1 coprecipitated with WT RASSF1A and increased in response to oxidative stress (Figure 3C). In contrast, Mst1 did not associate with the L308P mutant under any condition. K-Ras association with both forms of RASSF1A was comparable (Figure 3C). Size exclusion chromatography and subsequent immunoprecipitation experiments demonstrated that K-Ras, RASSF1A, and Mst1 were enriched and associated with one another in the same high-molecular-weight fractions isolated from hearts subjected to I/R, indicating trimolecular complex formation (Figures S3B–S3D). To test the requirement of each for Mst1 translocation, we first depleted endogenous K-Ras using an siRNA approach (Figure S3E). We found that K-Ras knockdown reduced Mst1 levels in mitochondria-enriched fractions following oxidative stress (Figure S3F). Similarly, expression of L308P RASSF1A significantly attenuated Mst1 translocation

to mitochondria following H₂O₂ stimulation, whereas expression of WT RASSF1A increased Mst1 present in mitochondria-enriched fractions compared to LacZ control (Figure 3D). Following I/R, Mst1 in mitochondria-enriched fractions was increased in WT hearts, while no increase was observed in Rassf1a⁻/⁻ hearts (Figures 3E and 3F). We also observed attenuated Mst1 activation in Rassf1a⁻/⁻ hearts after I/R (Figures 3G and 3H), although no difference in K-Ras activation was observed (Figure S3G). These results indicate that K-Ras and a functional RASSF1A are critical for translocation and activation of Mst1 in response to oxidative stress in the heart.

Mst1 Activates a Mitochondrial Death Pathway

We hypothesized that Mst1 promotes mitochondria-mediated apoptosis. Bcl-2 family proteins regulate mitochondrial integrity and apoptosis (Chipuk et al., 2010). We tested whether Mst1 associates with Bcl-2 family members. Overexpression studies showed no association between Mst1 and Bax, Bad, or Bcl-2 (Figures S4A–S4C). Conversely, we observed a clear association between endogenous Mst1 and ectopically expressed Bcl-xL (Figure S4D). We also detected an interaction between
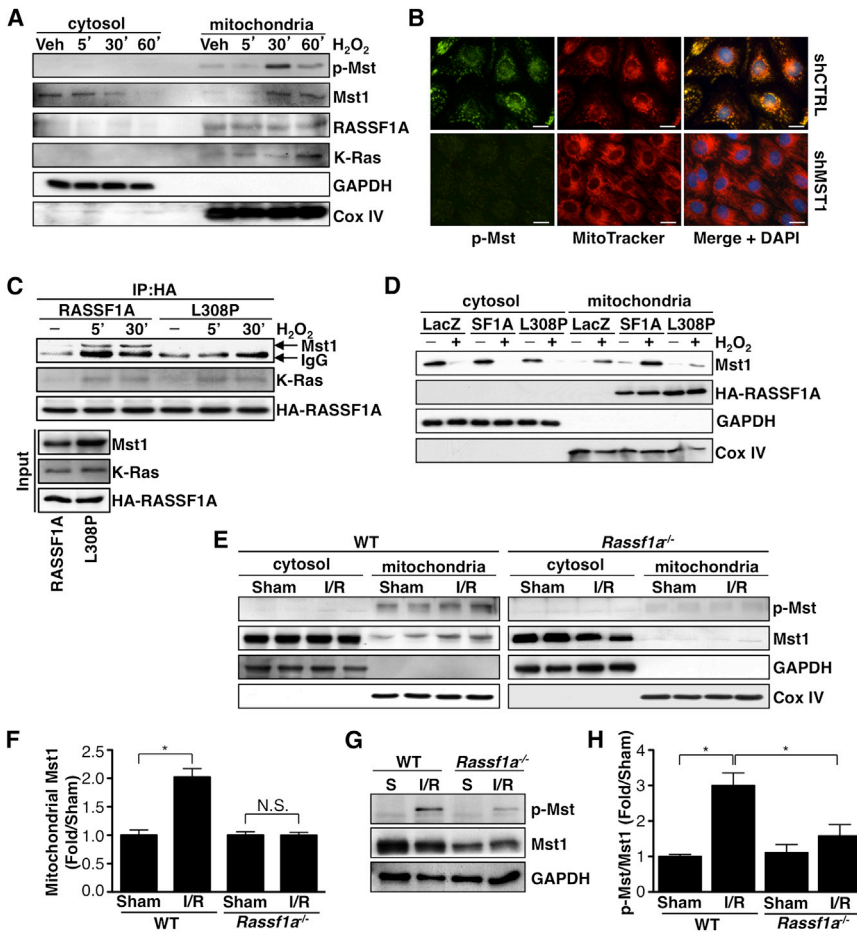
Figure 3. Mitochondrial Translocation of Mst1 Is Mediated by RASSF1A

(A) Cardiac myocytes were treated with vehicle or H_2O_2 (100 μM), and cells were harvested at 5, 15, 30, and 60 min. Subcellular fractionation was performed to obtain cytosolic (GAPDH)- and mitochondria (Cox IV)-enriched fractions.

(B) Localization of p-Mst1 (green) in cardiac myocytes transduced with either shCTRL or shMST1 adenovirus. Cells were treated with H_2O_2 (100 μM) for 30 min after knockdown. MitoTracker Red was used to visualize mitochondria. Scale bar, 20 μm.

(C) Interaction between RASSF1A and Mst1 is increased in response to oxidative stress. Cardiac myocytes were transduced with HA-RASSF1A or HA-RASSF1A(L308P) adenovirus and treated with vehicle or H_2O_2 (100 μM) for the times indicated. Samples were subjected to immunoprecipitation using anti-HA.

(D) The association between RASSF1A and Mst1 mediates Mst1 translocation. Cardiac myocytes were transduced with LacZ, HA-RASSF1A, or HA-RASSF1A(L308P) and treated with vehicle or H_2O_2 (100 μM) for 60 min, and cytosolic- and mitochondria-enriched fractions were prepared.

(E) Increased Mst1 in mitochondria-enriched fractions following I/R (30'/60') is attenuated in $Rassf1a^{-/-}$ hearts.

(F) Quantitation of results from I/R experiments; n = 3–4 per group. *p < 0.05. N.S., not significant.

(G) Mst1 phosphorylation by I/R (30'/60') is attenuated in $Rassf1a^{-/-}$ hearts.

(H) Quantitation of results from I/R experiments; n = 3–4 per group. *p < 0.05. Data are represented as mean ±SEM. See also Figure S3.

endogenous Mst1 and Bcl-xL in cardiac myocytes following oxidative stress (Figures 4A and S4E). We found this association was less prominent in (K59R)Dn-Mst1 compared to WT Mst1 and was driven by expression of K-Ras (Figures S4F and S4G). One mechanism by which Bcl-xL may exert its antiapoptotic effect is through inhibitory binding of Bax at the mitochondrial outer membrane (Edlich et al., 2011; Sedlak et al., 1995). We found that increased expression of Mst1 caused a decrease in Bcl-xL-Bax association (Figures 4B and 4C). Moreover, we observed increased levels of active Bax (6A7 epitope positive) in cardiac myocytes expressing Mst1 and in Mst1 transgenic (Tg) mouse hearts compared to controls, similar to cardiac myocytes treated with H_2O_2 (Figures 4D–4F and S4H). Mst1 expression in cardiac myocytes induced mitochondrial outer membrane permeabilization (MOMP), cytochrome c release, and activation of caspase-9 and caspase-3 (Figures 4G–4I), highlighting the mitochondria as a focal point of Mst1 action. Importantly we found that knockdown of Mst1 attenuated H_2O_2-induced apoptosis (Figure 4J), indicating the importance of endogenous Mst1. Furthermore, knockdown of endogenous Bcl-xL triggered increased apoptosis of cardiac myocytes, and caspase activation by Mst1 was abrogated in $bax^{-/-}bak^{-/-}$ mouse embryonic fibroblasts (MEFs), indicating that Bcl-xL and Bax are critical effectors of Mst1-induced apoptosis (Figures 4K and S4I).

Mst1 Phosphorylates Bcl-xL

Bcl-xL function is regulated by posttranslational modification. To determine whether Bcl-xL is phosphorylated by Mst1, we performed an in vitro kinase assay using recombinant Mst1 and Bcl-xL proteins and observed a clear signal indicating direct phosphorylation of Bcl-xL by Mst1 (Figure 5A). Phos-tag was used to detect phosphorylation of endogenous Bcl-xL and confirmed our in vitro results (Figure 5B). Phosphorylated Bcl-xL protein was submitted for mass spectrometry analysis. Approximately 70% sequence coverage of Bcl-xL was attained, and one phosphorylated residue, Ser14, was detected. This residue lies in the BH4 domain and α_1 helix of Bcl-xL (Figures S5A–S5C).

Previous work suggested that JNK could phosphorylate Ser62 of Bcl-xL, thereby limiting its ability to protect against apoptosis (Basu and Haldar, 2003). Our analysis did not identify Ser62 as a target of Mst1. To verify our screen, kinase reactions were performed using peptides corresponding to the α_1 helix region (containing Ser14) or control peptides (containing Ser62) and recombinant Mst1. Rapid incorporation of ATP[γ-^{32}P] was observed in the α_1 helix peptide, while no significant increase occurred with the control peptide (Figure S5D). Rabbit polyclonal antibody was generated using a p-Ser14 peptide (for sequence see Experimental Procedures), and its specificity for Ser14
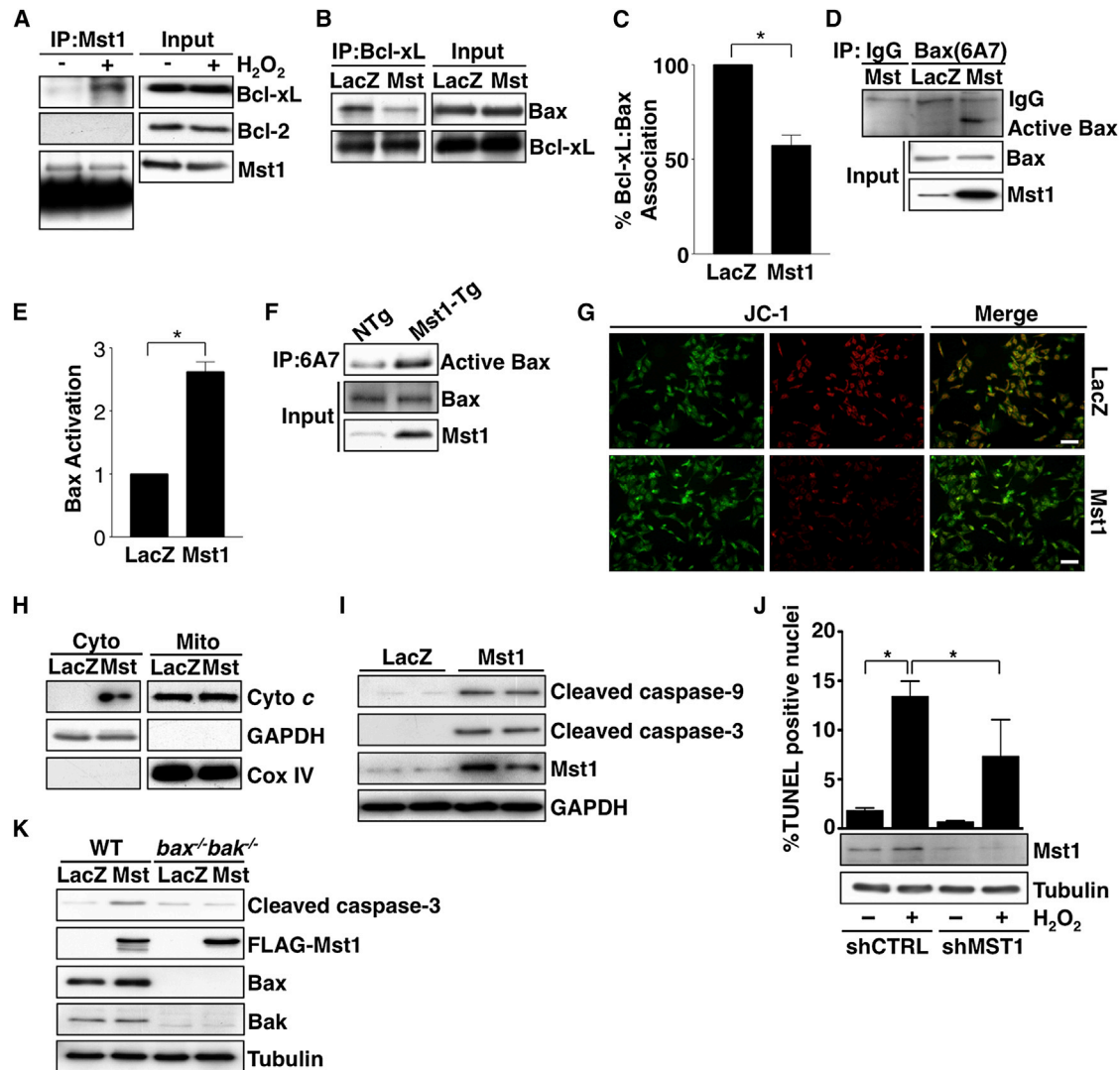
Figure 4. Mst1 Antagonizes Bcl-xL-Bax Association and Promotes Mitochondrial Apoptosis

(A) Oxidative stress promotes the interaction of endogenous Mst1 and Bcl-xL. Cardiac myocytes were treated with vehicle or H_2O_2 (100 μM) for 30 min. Immunocomplexes were precipitated using anti-Mst1 antibody.

(B) Mst1 expression decreases the association between endogenous Bcl-xL and Bax. Cardiac myocytes were transduced with LacZ or Mst1 adenovirus, and complexes were immunoprecipitated using anti-Bcl-xL antibody.

(C) Quantitation of Bcl-xL-Bax association; n = 3. *p < 0.05.

(D) Active Bax is increased following ectopic Mst1 expression. Cardiac myocytes were transduced with LacZ or Mst1 adenovirus, and the active conformation of Bax was precipitated using the monoclonal 6A7 anti-Bax antibody.

(E) Quantitation of Bax activation; n = 3. *p < 0.05.

(F) Active Bax is increased in Mst1-Tg mouse hearts compared to NTg controls.

(G) Mitochondrial membrane potential is decreased in cardiac myocytes expressing Mst1. Cells were incubated with JC-1 (10 μg/mL) for 15 min at 37°C to evaluate mitochondrial outer membrane integrity. Scale bar, 100 μm.

(H) Mst1 expression promotes cytochrome c accumulation in cytosol-enriched fractions in cardiac myocytes.

(I) Expression of Mst1 increases the cleaved form of caspase-9 and caspase-3 in cardiac myocytes.

(J) Knockdown of endogenous Mst1 attenuates oxidative stress-induced apoptosis. Cardiac myocytes were transduced with shCTRL or shMST1 adenovirus. Cells were then treated with vehicle or H_2O_2 (100 μM) and apoptosis evaluated by TUNEL. *p < 0.05. Data are represented as mean ±SEM.

(K) Mst1 expression induced caspase-3 activation in WT, but not $bax^{-/-}bak^{-/-}$, MEFs. See also Figure S4.

phosphorylation was confirmed (Figures S5E–S5G). Increased Mst1 expression in cardiac myocytes and mouse hearts caused increased Bcl-xL Ser14 phosphorylation compared to controls (Figures 5C and 5D). Bcl-xL from hearts subjected to I/R had

increased Ser14 phosphorylation while Ser62 phosphorylation was unchanged (Figure 5E). Importantly, Ser14 phosphorylation was attenuated in cardiac myocytes depleted of Mst1 and in Dn-Mst1-Tg hearts following I/R, providing additional evidence that

this mechanism translates in vivo (Figures S5H, S5I, and 5F). We also detected increased Ser14 phosphorylation in failing human hearts (Figure 5G). Using recombinant proteins in vitro, we found that ATP was critical for Mst1-induced attenuation of Bcl-xL-Bax binding (Figure 5H), indicating that phosphorylation is required.

To test the functional significance of Bcl-xL Ser14 phosphorylation, we generated two point mutations, Ser→Ala (S14A) and Ser→Asp (S14D), to prevent and mimic phosphorylation, respectively. Our data demonstrate that expression of Bcl-xL S14A significantly attenuated Mst1-induced apoptosis and showed greater protection compared to WT Bcl-xL. Conversely, we failed to observe protection by Bcl-xL S14D expression (Figure 5I). Similarly, WT Bcl-xL expression significantly decreased cell death in the presence of H_2O_2 and chelerythrine, a potent inducer of apoptosis in cardiac myocytes, and Bcl-xL S14A protected further still, while Bcl-xL S14D had no significant effect (Figure 5J). Myocardial expression of these constructs was attained through adenovirus injection into the left ventricular free wall (Figure S5J), and mice were subjected to I/R. We observed a significant reduction in infarct size in Bcl-xL WT and further protection in S14A-treated mice, while no difference was seen in the Bcl-xL S14D group compared to GFP control (Figures 5K–5M). Mechanistically, we observed attenuated association of Bcl-xL S14D mutant with endogenous Bax compared to Bcl-xL WT and S14A, suggesting that Bax association mediates its protective capacity (Figure S5K), whereas association with Bid and Bim were not changed. We also generated WT and S14A Bcl-xL protein in vitro and tested its ability to pull down recombinant Bax in the presence and absence of Mst1. We found that WT and S14A associated comparably with Bax in the absence of Mst1. However, following kinase reaction, Bax pulldown was decreased in WT compared to S14A (Figure S5L).

K-Ras Elicits Mst1-Dependent I/R Injury
To validate our findings in vivo, we employed genetic deletion mouse models of H- and K-Ras and tested their role in I/R injury. Disruption of K-Ras expression ($Kras^{+/-}$) led to a significant decrease in infarct size following I/R compared to WT littermates (Figures 6A–6D). Mst1 activation following I/R in WT hearts was significantly attenuated in $Kras^{+/-}$ hearts with no change in ERK1/2 or AKT activation (Figure 6E). In contrast, mice with heterozygous deficiency for H-Ras did not show a significant difference in infarct size after I/R (Figures 6F–6I). Mst1 activation was comparable in both WT and $Hras^{+/-}$ mouse hearts (Figure 6J). Interestingly, mice harboring homozygous deletion of H-Ras ($Hras^{-/-}$) showed a significant increase in infarct size after I/R and attenuated ERK1/2 activation compared to WT (Figures S6A–S6E). These data suggest a protective role for H-Ras but an injurious role for K-Ras during myocardial stress.

We generated K-Ras12V Tg mice and found a significant increase in infarct size in Tg hearts versus nontransgenic (NTg) littermates after I/R (Figures S6H–S6J). We also observed augmented Mst1 activation in Tg hearts suggesting that cardiac expression of K-Ras12V promotes Mst1 activity (Figure S6F). K-Ras12V was observed predominantly in mitochondria-enriched fractions of Tg hearts (Figure S6G). We generated bigenic mice by breeding K-Ras12V Tg with kinase-inactive (K59R) Mst1 Tg mice (K-Ras12V × Dn-Mst1) and determined

infarct size following I/R. Bigenic mice had a significantly reduced infarct size versus K-Ras12V Tg that was comparable to that of NTg mice (Figures S6H and S6I), further implicating Mst1 as a downstream mediator of K-Ras signaling during oxidative injury in the heart.

DISCUSSION

The Hippo pathway is highly conserved and a critical regulator of cell proliferation and survival. However, little is known regarding the subcellular localization of this kinase cascade (Yin et al., 2013). And while the core signaling components are well-described, proximal inputs and distal outputs that mediate cell death remain unclear. Similar to scaffold-mediated canonical MAPK signaling, our study identifies a signaling cassette that is present at mitochondria of cardiac myocytes. Stress elicits K-Ras activation and the subsequent interaction with RASSF1A, leading to RASSF1A-mediated engagement and activation of Mst1. We identify Bcl-xL as a novel Mst1 substrate that, when phosphorylated, decreases Bcl-xL-Bax interaction, increasing active Bax, MOMP, and cardiac myocyte apoptosis (Figure 6K). This cascade is distinct from the prosurvival activation of ERK1/2 and PI3K/AKT driven by H-Ras.

Mst1 is an evolutionarily conserved stress responsive kinase that modulates cell growth, proliferation, and apoptosis. Several targets of Mst1 have been identified, yet the mechanism underlying Mst1-induced cell death remains unclear. We identify Ser14 of Bcl-xL as a direct target of Mst1 phosphorylation. Previous work reported that JNK-dependent phosphorylation of Bcl-xL at Ser62 could promote apoptosis (Basu and Haldar, 2003). We did not observe Ser62 phosphorylation by Mst1 by mass spectrometry analysis, indicating the likelihood of kinase/cell-type/tissue specificity of Bcl-xL phosphorylation. Moreover, our results demonstrate that Bcl-xL phosphorylation is important for Mst1-induced apoptosis and present a substrate distinct from canonical Hippo signaling, commonly characterized by the phosphorylation of Lats/Yap.

The interaction between Bcl-2 family proteins regulates MOMP and apoptosis; however, the underlying mechanisms remain controversial and warrant continued investigation. In response to insult, the effector proteins Bax and Bak undergo conformational changes, insert/oligomerize in the mitochondrial outer membrane, and induce MOMP (Chipuk et al., 2010; Gavathiotis et al., 2008). Whether antiapoptotic Bcl-2 proteins prevent death by associating with BH3-only proteins to prevent Bax/Bak activation (the "direct-activation" model; Kim et al., 2006; Kuwana et al., 2002; Letai et al., 2002; Willis et al., 2007), through direct association with Bax/Bak (the "embedded together" model; Leber et al., 2007, 2010), or some combination of the two remains unclear. An elegant study from Green and colleagues recently provided strong evidence for a "unified" model of intrinsic apoptosis (Llambi et al., 2011) that incorporates and further refines the previously proposed mechanisms. Here, Llambi et al. (2011) describe two "modes" of antiapoptotic Bcl-2 protein function: the first demonstrates that Bcl-xL (and presumably Bcl-2) binds and prevents BH3-only activator function, while the second demonstrates direct association of Bcl-xL and Bax/Bak to prevent MOMP. Interestingly, the latter mode
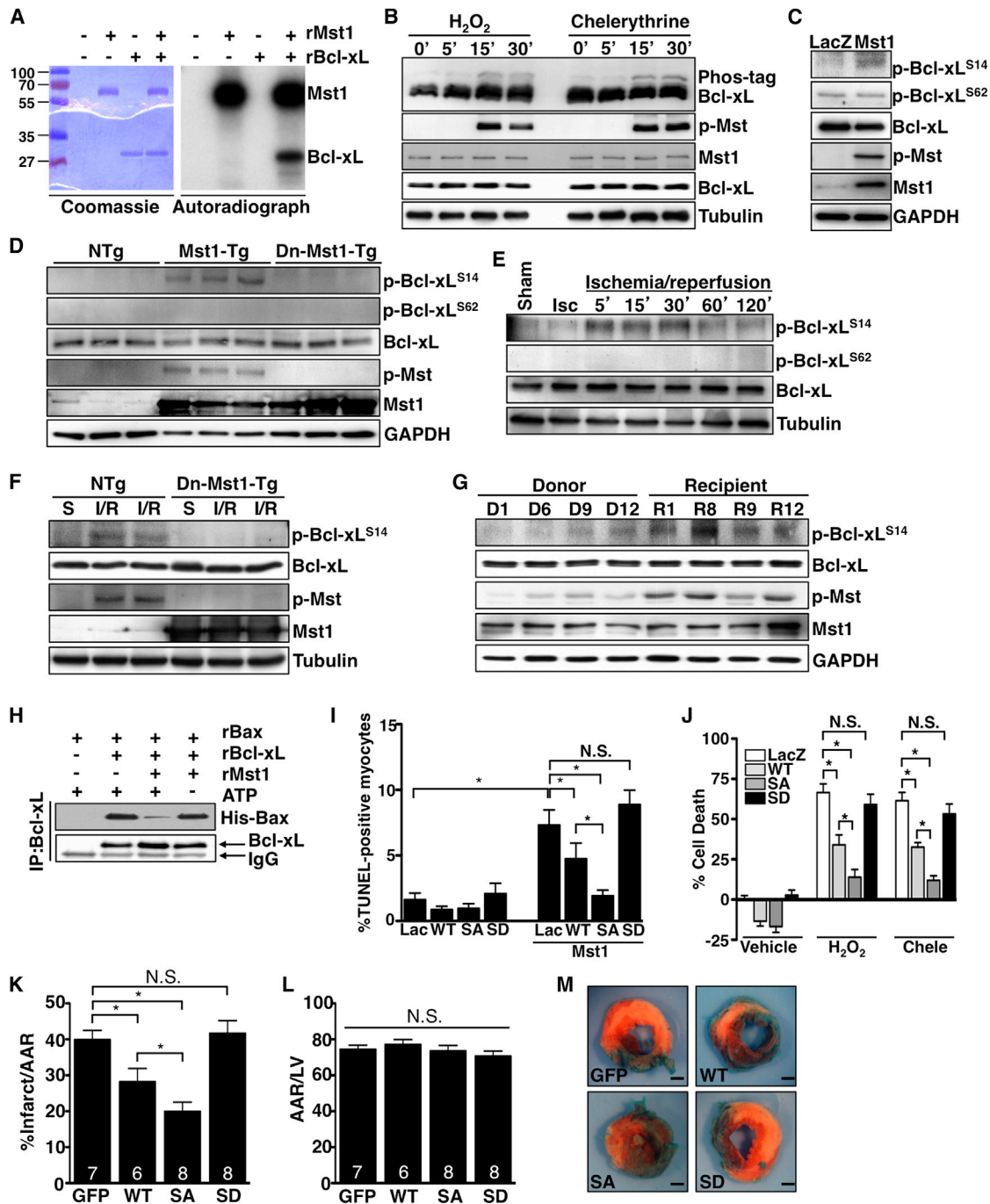
Figure 5. Mst1 Phosphorylates Bcl-xL at Serine 14

(A) Autoradiograph (right panel) demonstrating direct phosphorylation of Bcl-xL by Mst1 and the corresponding Coomassie-stained gel (left panel). In vitro kinase reaction was performed at 30°C for 30 min using recombinant human Mst1 and Bcl-xL proteins.

(B) Stress induces phosphorylation of endogenous Bcl-xL. Cardiac myocytes were treated with H_2O_2 (100 µM) or chelerythrine (10 µM) for the times indicated. Cell lysates were analyzed by Phos-tag to visualize the shifted phosphorylated species.

(C) Increased Mst1 expression promotes Bcl-xL phosphorylation at Ser14. Cardiac myocytes were transduced with LacZ or Mst1 adenovirus, and phosphorylation of Ser14 and Ser62 was detected using phospho-specific antibodies.

(D) Bcl-xL phosphorylation in hearts of NTg, Mst1-Tg, and Dn-Mst1-Tg mice.

(E) Phosphorylation of Bcl-xL at Ser14 is increased during I/R. WT mice were subjected to sham operation, 30 min ischemia (Isc), or ischemia followed by various times of reperfusion.

(F) NTg and Dn-Mst1-Tg mice were subjected to sham or I/R (30'/30') operation, and heart homogenates were probed for Bcl-xL Ser14 phosphorylation.

(legend continued on next page)

(direct binding to Bax) was shown to be more effective at preventing MOMP. Bcl-xL contains a C-terminal transmembrane sequence that targets it to the mitochondrial outer membrane (Kaufmann et al., 2003). Recent work from the Youle group has demonstrated that Bcl-xL binds to Bax at the mitochondrial outer membrane and mediates a constant retro-translocation of Bax away from mitochondria (Edlich et al., 2011). We believe our current findings are consistent with the "unified" paradigm in that Bcl-xL is present at the mitochondria outer membrane and is phosphorylated by Mst1 in response to oxidative stress. Moreover, our results suggest a plausible mechanism describing how Bcl-xL and Bax dissociation occurs.

Prior studies have demonstrated that the BH1-3 domains (Yin et al., 1994; Zha et al., 1996) and BH4 domain (Ding et al., 2010) of Bcl-xL/Bcl-2 are important for interaction with Bax. Ser14 resides in the α_1 helix and BH4 domain of Bcl-xL and is conserved among mammalian Bcl-xL isoforms, but it is not present in the corresponding BH4 domain of Bcl-2. However, prior work has demonstrated that mutation of Val15→Glu disrupts Bcl-2 interaction with Bax (Hirotani et al., 1999). The V15E mutation introduces a negative charge that could mimic phosphorylation and suggests a similar BH4-regulated mechanism of Bax binding.

Both apoptotic and necrotic mechanisms contribute to tissue injury suffered in response to acute myocardial ischemia and reperfusion. Recent work has demonstrated that Bcl-2 family proteins can alter mitochondrial morphology and dynamics by modulating fission and fusion processes (Hoppins et al., 2011). Furthermore, the ability of Bax to target mitofusin 2 and promote mitochondrial fusion may facilitate necrosis of cardiac myocytes during myocardial infarction (Whelan et al., 2012). Taken together, there is growing evidence that Bcl-2 family proteins regulate complex pathways that impinge upon cell death at mitochondria. Our findings demonstrate that the Bcl-xL S14A mutant affords greater protection in the heart, more effectively prevents apoptosis, and increases cell viability versus WT Bcl-xL. We speculate that this is due to inhibition of apoptosis and necrosis, and future efforts will address this possibility. Our recent work has demonstrated that Mst1 phosphorylates Beclin1 during chronic ischemia, thereby promoting the interaction of Beclin1 and Bcl-2 and inhibiting autophagy (Maejima et al., 2013). While this signaling event may indirectly lead to activation of Bax, our current study demonstrates direct Bax activation in response to Bcl-xL phosphorylation by Mst1.

Differences in Ras isoform signaling have been associated with differences in subcellular localization (Hancock, 2003). Although our assessment was not quantitative or comprehensive, we found that both H-Ras and K-Ras are present in microsome/SR-enriched fractions; however, only K-Ras was detected in the mitochondria-enriched fraction of cardiac myocytes. We speculate that this selectivity may be due to signaling, chaperones, or a mitochondrial membrane composition that is unique to cardiac myocytes, and investigation into these possibilities is ongoing. Mitochondria generate reactive oxygen species following injury, and Ras proteins are known targets of oxidation, which can promote their activation (Lander et al., 1995). We observed selective oxidation and activation of K-Ras in cardiac myocytes and speculate that location of Ras isoforms influences their engagement with effectors and subsequent downstream signaling in agreement with the Ras literature.

Due to their prominent role in cancer, Ras proteins are targets of great therapeutic interest (Downward, 2003). While small-molecule competitive inhibition of ATP is an effective means of preventing kinase function, this approach is vastly more difficult for small GTPases due to their picomolar binding affinity for GTP (Vigil et al., 2010). Consequently, research has focused on proximal regulators of Ras membrane association, including farnesyl-tranferase inhibition, as well as downstream effector pathways. Along these lines, recent work demonstrated that small molecule targeting can effectively disrupt the interaction between the farnesyl tail of K-Ras and PDEδ, thereby preventing plasma membrane localization and oncogenic downstream signaling (Zimmermann et al., 2013). In light of our current findings, we propose that the inhibition of K-Ras/RASSF1A/Mst1 complex formation, perhaps by targeting RASSF1A rather than K-Ras or directly targeting Bcl-xL phosphorylation, could have therapeutic benefits for the treatment of myocardial injury.

EXPERIMENTAL PROCEDURES

Genetically Modified Mice

K-Ras12V Tg mice were generated (FVB/N background) using cDNA of human myc-K-Ras12V driven by the α-myosin heavy chain promoter (J. Robbins, University of Cincinnati) to achieve cardiac-specific expression. $Kras^{+/-}$, $Hras^{+/-}$, $Rassf1a^{-/-}$, Mst1-Tg, and Dn-Mst1-Tg mice have been described previously (Esteban et al., 2001; Johnson et al., 1997; van der Weyden et al., 2005; Yamamoto et al., 2003). Dn-Mst1-Tg and K-Ras12V Tg mice were bred to generate bigenic mice. Mice were housed in a temperature-controlled environment with 12 hr light/dark cycles where they received food and water ad libitum.

(G) Bcl-xL Ser14 phosphorylation is increased in failing human hearts. Immunoblot of Bcl-xL and Mst1 phosphorylation in donor (healthy; D1, 6, 9, and 12) and recipient (diseased; R1, 8, 9, and 12) human heart tissue samples.

(H) Mst1 inhibits the association between Bcl-xL and Bax in vitro. Recombinant Bcl-xL was incubated with recombinant Mst1 in the presence or absence of ATP prior to incubation with recombinant Bax protein and subsequent immunoprecipitation using anti-Bcl-xL antibody.

(I) Bcl-xL phosphomimetic mutant showed impaired protection against Mst1-induced apoptosis. Cardiac myocytes were transduced with LacZ, wild-type Bcl-xL (WT), Bcl-xL Ser[14]→Ala (SA), or Bcl-xL Ser[14]→Asp (SD) with or without Mst1 and TUNEL was performed after 48 hr, n = 3. *p < 0.05. N.S., not significant.

(J) Bcl-xL phosphomimetic mutant had impaired protection against cardiac myocyte death. Myocytes were transduced with adenovirus as described in (I) prior to treatment with H_2O_2 (100 μM), chelerythrine (10 μM), or vehicle for 24 hr. Cell Titer Blue assay was used to quantitate cell viability; n = 3. *p < 0.05. N.S., not significant.

(K) Hearts of WT mice were transduced with adenovirus. Mice were subjected to I/R (30′/24hr), and the left ventricle was sectioned and incubated with 1% TTC to visualize infarct (pale white). Alcian blue was used to demarcate area at risk (AAR, red) from nonischemic tissue (blue). Quantitation of infarct as a percentage of area at risk (AAR). *p < 0.05.

(L) Quantitation of AAR as a percentage of left ventricular mass. N.S., not significant.

(M) Representative images demonstrating infarct size of treatment groups. Scale bar, 1 mm. Data are represented as mean ±SEM. See also Figure S5.
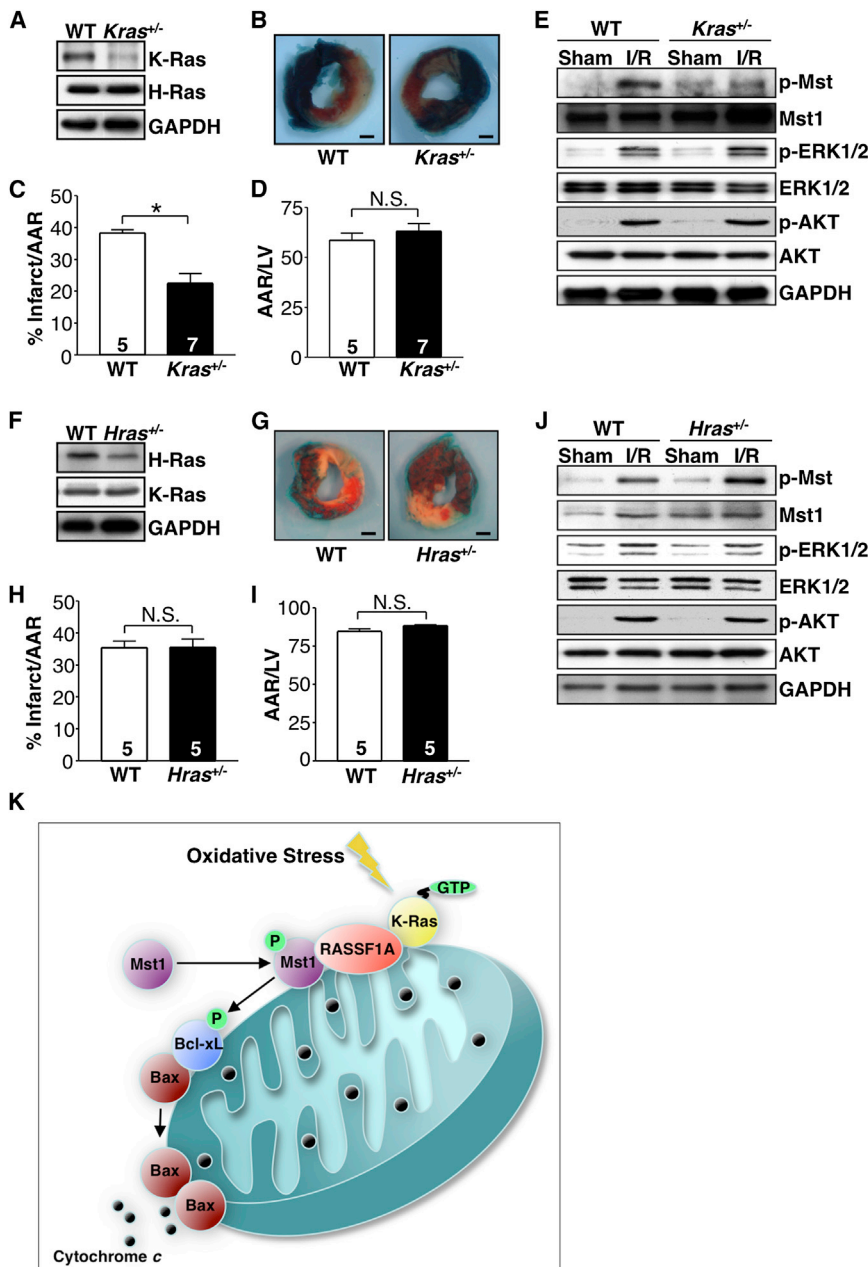
Figure 6. $Kras^{+/-}$ Mice Are Protected against I/R Injury

(A) Representative immunoblot showing reduced K-Ras expression in the $Kras^{+/-}$ mouse heart.

(B) Representative images demonstrating reduced infarct size in $Kras^{+/-}$ hearts. Scale bar, 1 mm.

(C) Quantitation of infarct as a percentage of AAR. *p < 0.05.

(D) Quantitation of AAR as a percentage of left ventricular mass. N.S., not significant.

(E) Representative immunoblot demonstrating attenuated Mst1 activation in $Kras^{+/-}$ hearts after I/R. Mice were subjected to sham or I/R (30′/60′) and ventricular extracts were analyzed.

(F) Representative immunoblot showing reduced H-Ras expression in $Hras^{+/-}$ mouse hearts.

(G) Representative images demonstrating no change in infarct size in $Hras^{+/-}$ hearts. Scale bar, 1 mm.

(H) Quantitation of infarct as a percentage of AAR. N.S., not significant.

(I) Quantitation of AAR as a percentage of left ventricle mass. N.S., not significant. Data are represented as mean ±SEM.

(J) Representative immunoblot demonstrating unaltered Mst1 activation in $Hras^{+/-}$ hearts after I/R. Mice were subjected to sham or I/R and analyzed as described in (E).

(K) Schema summarizing our working hypothesis. See also Figure S6.

Adenovirus Injection

Adenovirus (1×10^9 pfu) was administered by direct injection to the LV free wall (two sites, 20 μl/site) as described previously (Belke et al., 2006). I/R was performed 2 days after injection.

Subcellular Fractionation

Isolated mouse ventricles or cardiac myocytes were homogenized and fractionated as described previously (Ago et al., 2010).

RBD Pulldown Assay

Lysates were incubated with Raf-1 RBD agarose (Upstate) according to manufacturer's instructions.

Detection of Thiolated Cysteines

Lysates were prepared using lysis buffer containing 200 μmol/L biotinylated iodoacetamide (Sigma) and incubated at room temperature for 30 min. Lysates were cleared by centrifugation and the supernatant incubated with streptavidin-agarose beads (Sigma) for 2 hr at 4°C. Beads were washed in lysis buffer containing 200 μmol/L biotinylated-IAM and subjected to SDS-PAGE.

All protocols concerning the use of animals were approved by the Institutional Animal Care and Use Committee at New Jersey Medical School, Rutgers.

Cell Cultures

Primary cultures of ventricular cardiac myocytes were prepared from 1-day-old Crl: (WI)BR-Wistar rats (Harlan Laboratories, Somerville) and maintained in culture as described previously (Sadoshima and Izumo, 1993). $bax^{-/-}bak^{-/-}$ MEFs (kindly provided by Dr. Richard N. Kitsis, Albert Einstein University), HEK293, COS-7, and C2C12 cells were maintained at 37°C with 5% CO_2 in Dulbecco's modified Eagle's medium supplemented with 10% fetal bovine serum.

Adenoviral Constructs

Recombinant adenovirus vectors for overexpression and short hairpin RNA-mediated gene silencing were constructed as described previously (Matsui et al., 2008).

JC-1 Staining

Cardiac myocytes were stained with 5,5′,6,6′-tetrachloro-1,1′ 3,3′-tetraethyl-benzimidazolocarbocyanine iodide (JC-1) according to the manufacturer's instructions (ImmunoChemistry Technologies).

Evaluation of Apoptosis

DNA fragmentation was detected in cardiac myocytes using TUNEL as described previously (Yamamoto et al., 2003). Nuclear density was determined by counting DAPI-stained nuclei in 20 different fields for each sample.

Molecular Cell

Mst1 Antagonizes Bcl-xL Function

CellPress

Cell Viability Assay

Cell viability was measured by Cell Titer Blue assay (Promega) according to the manufacturer's protocol.

Statistical Analysis

All data are reported as mean ±SEM. Statistical analyses between groups were done by one-way ANOVA, and differences among group means were evaluated using the Newman-Keuls post hoc test. Student's t test was used between data pairs. A p value less than 0.05 was considered significant.

SUPPLEMENTAL INFORMATION

Supplemental Information includes six figures and Supplemental Experimental Procedures and can be found with this article online at http://dx.doi.org/10.1016/j.molcel.2014.04.007.

REFERENCES

Ago, T., Kuroda, J., Pain, J., Fu, C., Li, H., and Sadoshima, J. (2010). Upregulation of Nox4 by hypertrophic stimuli promotes apoptosis and mitochondrial dysfunction in cardiac myocytes. Circ. Res. *106*, 1253–1264.

Avruch, J., Xavier, R., Bardeesy, N., Zhang, X.F., Praskova, M., Zhou, D., and Xia, F. (2009). Rassf family of tumor suppressor polypeptides. J. Biol. Chem. *284*, 11001–11005.

Basu, A., and Haldar, S. (2003). Identification of a novel Bcl-xL phosphorylation site regulating the sensitivity of taxol- or 2-methoxyestradiol-induced apoptosis. FEBS Lett. *538*, 41–47.

Belke, D.D., Gloss, B., Hollander, J.M., Swanson, E.A., Duplain, H., and Dillmann, W.H. (2006). In vivo gene delivery of HSP70i by adenovirus and adeno-associated virus preserves contractile function in mouse heart following ischemia-reperfusion. Am. J. Physiol. Heart Circ. Physiol. *291*, H2905–H2910.

Chipuk, J.E., Moldoveanu, T., Llambi, F., Parsons, M.J., and Green, D.R. (2010). The BCL-2 family reunion. Mol. Cell *37*, 299–310.

Del Re, D.P., Matsuda, T., Zhai, P., Gao, S., Clark, G.J., Van Der Weyden, L., and Sadoshima, J. (2010). Proapoptotic Rassf1A/Mst1 signaling in cardiac fibroblasts is protective against pressure overload in mice. J. Clin. Invest. *120*, 3555–3567.

Ding, J., Zhang, Z., Roberts, G.J., Falcone, M., Miao, Y., Shao, Y., Zhang, X.C., Andrews, D.W., and Lin, J. (2010). Bcl-2 and Bax interact via the BH1-3 groove-BH3 motif interface and a novel interface involving the BH4 motif. J. Biol. Chem. *285*, 28749–28763.

Downward, J. (2003). Targeting RAS signalling pathways in cancer therapy. Nat. Rev. Cancer *3*, 11–22.

Edlich, F., Banerjee, S., Suzuki, M., Cleland, M.M., Arnoult, D., Wang, C., Neutzner, A., Tjandra, N., and Youle, R.J. (2011). Bcl-x(L) retrotranslocates Bax from the mitochondria into the cytosol. Cell *145*, 104–116.

Esteban, L.M., Vicario-Abejón, C., Fernández-Salguero, P., Fernández-Medarde, A., Swaminathan, N., Yienger, K., Lopez, E., Malumbres, M., McKay, R., Ward, J.M., et al. (2001). Targeted genomic disruption of H-ras and N-ras, individually or in combination, reveals the dispensability of both loci for mouse growth and development. Mol. Cell. Biol. *21*, 1444–1452.

Gavathiotis, E., Suzuki, M., Davis, M.L., Pitter, K., Bird, G.H., Katz, S.G., Tu, H.C., Kim, H., Cheng, E.H., Tjandra, N., and Walensky, L.D. (2008). BAX activation is initiated at a novel interaction site. Nature *455*, 1076–1081.

Gavathiotis, E., Reyna, D.E., Davis, M.L., Bird, G.H., and Walensky, L.D. (2010). BH3-triggered structural reorganization drives the activation of proapoptotic BAX. Mol. Cell *40*, 481–492.

Graves, J.D., Gotoh, Y., Draves, K.E., Ambrose, D., Han, D.K., Wright, M., Chernoff, J., Clark, E.A., and Krebs, E.G. (1998). Caspase-mediated activation and induction of apoptosis by the mammalian Ste20-like kinase Mst1. EMBO J. *17*, 2224–2234.

Hancock, J.F. (2003). Ras proteins: different signals from different locations. Nat. Rev. Mol. Cell Biol. *4*, 373–384.

Hirotani, M., Zhang, Y., Fujita, N., Naito, M., and Tsuruo, T. (1999). NH2-terminal BH4 domain of Bcl-2 is functional for heterodimerization with Bax and inhibition of apoptosis. J. Biol. Chem. *274*, 20415–20420.

Hoppins, S., Edlich, F., Cleland, M.M., Banerjee, S., McCaffery, J.M., Youle, R.J., and Nunnari, J. (2011). The soluble form of Bax regulates mitochondrial fusion via MFN2 homotypic complexes. Mol. Cell *41*, 150–160.

Johnson, L., Greenbaum, D., Cichowski, K., Mercer, K., Murphy, E., Schmitt, E., Bronson, R.T., Umanoff, H., Edelmann, W., Kucherlapati, R., and Jacks, T. (1997). K-ras is an essential gene in the mouse with partial functional overlap with N-ras. Genes Dev. *11*, 2468–2481.

Karnoub, A.E., and Weinberg, R.A. (2008). Ras oncogenes: split personalities. Nat. Rev. Mol. Cell Biol. *9*, 517–531.

Kaufmann, T., Schlipf, S., Sanz, J., Neubert, K., Stein, R., and Borner, C. (2003). Characterization of the signal that directs Bcl-x(L), but not Bcl-2, to the mitochondrial outer membrane. J. Cell Biol. *160*, 53–64.

Kim, H., Rafiuddin-Shah, M., Tu, H.C., Jeffers, J.R., Zambetti, G.P., Hsieh, J.J., and Cheng, E.H. (2006). Hierarchical regulation of mitochondrion-dependent apoptosis by BCL-2 subfamilies. Nat. Cell Biol. *8*, 1348–1358.

Kuwana, T., Mackey, M.R., Perkins, G., Ellisman, M.H., Latterich, M., Schneiter, R., Green, D.R., and Newmeyer, D.D. (2002). Bid, Bax, and lipids cooperate to form supramolecular openings in the outer mitochondrial membrane. Cell *111*, 331–342.

Lander, H.M., Ogiste, J.S., Teng, K.K., and Novogrodsky, A. (1995). p21ras as a common signaling target of reactive free radicals and cellular redox stress. J. Biol. Chem. *270*, 21195–21198.

Leber, B., Lin, J., and Andrews, D.W. (2007). Embedded together: the life and death consequences of interaction of the Bcl-2 family with membranes. Apoptosis *12*, 897–911.

Leber, B., Lin, J., and Andrews, D.W. (2010). Still embedded together binding to membranes regulates Bcl-2 protein interactions. Oncogene *29*, 5221–5230.

Letai, A., Bassik, M.C., Walensky, L.D., Sorcinelli, M.D., Weiler, S., and Korsmeyer, S.J. (2002). Distinct BH3 domains either sensitize or activate mitochondrial apoptosis, serving as prototype cancer therapeutics. Cancer Cell *2*, 183–192.

Lips, D.J., Bueno, O.F., Wilkins, B.J., Purcell, N.H., Kaiser, R.A., Lorenz, J.N., Voisin, L., Saba-El-Leil, M.K., Meloche, S., Pouysségur, J., et al. (2004). MEK1-ERK2 signaling pathway protects myocardium from ischemic injury in vivo. Circulation *109*, 1938–1941.

Llambi, F., Moldoveanu, T., Tait, S.W., Bouchier-Hayes, L., Temirov, J., McCormick, L.L., Dillon, C.P., and Green, D.R. (2011). A unified model of mammalian BCL-2 protein family interactions at the mitochondria. Mol. Cell *44*, 517–531.

Maejima, Y., Kyoi, S., Zhai, P., Liu, T., Li, H., Ivessa, A., Sciarretta, S., Del Re, D.P., Zablocki, D.K., Hsu, C.P., et al. (2013). Mst1 inhibits autophagy by promoting the interaction between Beclin1 and Bcl-2. Nat. Med. *19*, 1478–1488.

Matsui, Y., Nakano, N., Shao, D., Gao, S., Luo, W., Hong, C., Zhai, P., Holle, E., Yu, X., Yabuta, N., et al. (2008). Lats2 is a negative regulator of myocyte size in the heart. Circ. Res. *103*, 1309–1318.

Moldoveanu, T., Follis, A.V., Kriwacki, R.W., and Green, D.R. (2014). Many players in BCL-2 family affairs. Trends Biochem. Sci. *39*, 101–111.

Moodie, S.A., Willumsen, B.M., Weber, M.J., and Wolfman, A. (1993). Complexes of Ras.GTP with Raf-1 and mitogen-activated protein kinase kinase. Science *260*, 1658–1661.

Odashima, M., Usui, S., Takagi, H., Hong, C., Liu, J., Yokota, M., and Sadoshima, J. (2007). Inhibition of endogenous Mst1 prevents apoptosis and cardiac dysfunction without affecting cardiac hypertrophy after myocardial infarction. Circ. Res. *100*, 1344–1352.

Pan, D. (2010). The hippo signaling pathway in development and cancer. Dev. Cell *19*, 491–505.

Rodriguez-Viciana, P., Warne, P.H., Dhand, R., Vanhaesebroeck, B., Gout, I., Fry, M.J., Waterfield, M.D., and Downward, J. (1994). Phosphatidylinositol-3-OH kinase as a direct target of Ras. Nature *370*, 527–532.

Sadoshima, J., and Izumo, S. (1993). Molecular characterization of angiotensin II—induced hypertrophy of cardiac myocytes and hyperplasia of cardiac fibroblasts. Critical role of the AT1 receptor subtype. Circ. Res. *73*, 413–423.

Sedlak, T.W., Oltvai, Z.N., Yang, E., Wang, K., Boise, L.H., Thompson, C.B., and Korsmeyer, S.J. (1995). Multiple Bcl-2 family members demonstrate selective dimerizations with Bax. Proc. Natl. Acad. Sci. USA *92*, 7834–7838.

Simpson, P.J., and Lucchesi, B.R. (1987). Free radicals and myocardial ischemia and reperfusion injury. J. Lab. Clin. Med. *110*, 13–30.

van der Weyden, L., Tachibana, K.K., Gonzalez, M.A., Adams, D.J., Ng, B.L., Petty, R., Venkitaraman, A.R., Arends, M.J., and Bradley, A. (2005). The RASSF1A isoform of RASSF1 promotes microtubule stability and suppresses tumorigenesis. Mol. Cell. Biol. *25*, 8356–8367.

Vigil, D., Cherfils, J., Rossman, K.L., and Der, C.J. (2010). Ras superfamily GEFs and GAPs: validated and tractable targets for cancer therapy? Nat. Rev. Cancer *10*, 842–857.

Vojtek, A.B., Hollenberg, S.M., and Cooper, J.A. (1993). Mammalian Ras interacts directly with the serine/threonine kinase Raf. Cell *74*, 205–214.

Vos, M.D., Ellis, C.A., Bell, A., Birrer, M.J., and Clark, G.J. (2000). Ras uses the novel tumor suppressor RASSF1 as an effector to mediate apoptosis. J. Biol. Chem. *275*, 35669–35672.

Warne, P.H., Viciana, P.R., and Downward, J. (1993). Direct interaction of Ras and the amino-terminal region of Raf-1 in vitro. Nature *364*, 352–355.

Whelan, R.S., Konstantinidis, K., Wei, A.C., Chen, Y., Reyna, D.E., Jha, S., Yang, Y., Calvert, J.W., Lindsten, T., Thompson, C.B., et al. (2012). Bax regulates primary necrosis through mitochondrial dynamics. Proc. Natl. Acad. Sci. USA *109*, 6566–6571.

Willis, S.N., Fletcher, J.I., Kaufmann, T., van Delft, M.F., Chen, L., Czabotar, P.E., Ierino, H., Lee, E.F., Fairlie, W.D., Bouillet, P., et al. (2007). Apoptosis initiated when BH3 ligands engage multiple Bcl-2 homologs, not Bax or Bak. Science *315*, 856–859.

Yamamoto, S., Yang, G., Zablocki, D., Liu, J., Hong, C., Kim, S.J., Soler, S., Odashima, M., Thaisz, J., Yehia, G., et al. (2003). Activation of Mst1 causes dilated cardiomyopathy by stimulating apoptosis without compensatory ventricular myocyte hypertrophy. J. Clin. Invest. *111*, 1463–1474.

Yin, X.M., Oltvai, Z.N., and Korsmeyer, S.J. (1994). BH1 and BH2 domains of Bcl-2 are required for inhibition of apoptosis and heterodimerization with Bax. Nature *369*, 321–323.

Yin, F., Yu, J., Zheng, Y., Chen, Q., Zhang, N., and Pan, D. (2013). Spatial organization of Hippo signaling at the plasma membrane mediated by the tumor suppressor Merlin/NF2. Cell *154*, 1342–1355.

Zha, H., Aimé-Sempé, C., Sato, T., and Reed, J.C. (1996). Proapoptotic protein Bax heterodimerizes with Bcl-2 and homodimerizes with Bax via a novel domain (BH3) distinct from BH1 and BH2. J. Biol. Chem. *271*, 7440–7444.

Zhang, X.F., Settleman, J., Kyriakis, J.M., Takeuchi-Suzuki, E., Elledge, S.J., Marshall, M.S., Bruder, J.T., Rapp, U.R., and Avruch, J. (1993). Normal and oncogenic p21ras proteins bind to the amino-terminal regulatory domain of c-Raf-1. Nature *364*, 308–313.

Zhao, B., Tumaneng, K., and Guan, K.L. (2011). The Hippo pathway in organ size control, tissue regeneration and stem cell self-renewal. Nat. Cell Biol. *13*, 877–883.

Zimmermann, G., Papke, B., Ismail, S., Vartak, N., Chandra, A., Hoffmann, M., Hahn, S.A., Triola, G., Wittinghofer, A., Bastiaens, P.I., and Waldmann, H. (2013). Small molecule inhibition of the KRAS-PDEδ interaction impairs oncogenic KRAS signalling. Nature *497*, 638–642.